Developmental aspects of biomineralisation in the Polynesian pearl oyster *Pinctada margaritifera* var. *cumingii*

Lydie MAO CHE[a,b], Stjepko GOLUBIC[c], Thérèse LE CAMPION-ALSUMARD[d], Claude PAYRI[a]*

[a] Laboratoire d'écologie marine, université de Polynésie française, BP 6570, Faaa, Tahiti, French Polynesia

[b] Service des ressources marines, BP 20, Papeete, Tahiti, French Polynesia

[c] Department of Biology, Boston University, 5 Cummington Street, Boston, MA 02125, USA

[d] Centre d'océanologie de Marseille, UMR CNRS 6540, université de la Méditerranée, rue de la Batterie-des-Lions, 13007 Marseille, France

Abstract – The shell biomineralisation with special reference to the nacreous region is observed during the development of the Polynesian pearl oyster. Ultrastructural changes were studied and timed for the first time from planktonic larval shells to two-year-old adult shells. During the first two weeks following fertilization, the prodissoconch-I shell structure is undifferentiated and uniformly granular. The prodissoconch-II stage which develops during the next two weeks acquires a columnar organization. Metamorphosis is characterized by the formation of the dissoconch shell with all the elements of an adult shell and marks the onset of the development of the nacre. Nucleation starts within an organic matrix from point sources forming 'crystal germs' which expand circularly until they fuse. The orientation of the contour lines of scalariform growth margins indicates the direction of shell growth. Five zones of growth (Z) were characterized. One-month-old shells show a homogenous zone, without particular figures (Z0). The contour lines are initially parallel to the growing shell edge (Z1), later becoming labyrinthic (finger prints, Z2) or perpendicular to the edge (Z3). A fourth zone (Z4) characterized by spiral growth and associated with the shell thickening is observed later in the umbo region. This development results from a gradual lowering of the rate of mineralisation over time and from changes in growth pattern from a predominant increase in size, shifting toward an increase in the thickness of the shell. The mineralisation patterns of the shells from larvae reared in hatchery conditions and larvae from the field appear similar. The use of quantified information on shape, density, and distribution of nucleation sites as an indicator of growth conditions is discussed. © 2001 Ifremer/CNRS/IRD/Éditions scientifiques et médicales Elsevier SAS

Résumé – Biominéralisation de l'huître perlière polynésienne *Pinctada margaritifera* var. *cumingii* au cours de son développement. La biominéralisation de la coquille de l'huître perlière de Polynésie française, en particulier celle de sa partie nacrée, est étudiée au cours du développement du bivalve. Les changements de l'ultrastructure de sa coquille sont suivis, pour la première fois, du stade larvaire planctonique (prodissoconque I et II) au stade adulte de deux ans (dissoconque). Durant les deux premières semaines qui suivent la ponte, la prodissoconque I présente une structure granuleuse, sans aucune organisation apparente. La prodissoconque II qui se développe durant les deux semaines suivantes a une organisation en colonne. Au moment de la métamorphose, une dissoconque s'ajoute à la coquille larvaire. La fixation des larves planctoniques marque ainsi la mise en place de la couche nacrée. La taille, la densité et la

*Correspondence and reprints.
E-mail address: payri@upf.pf (C. PAYRI).

distribution des sites de nucléation des carbonates évoluent au cours du temps et dans différentes régions de la coquille. La nucléation prend naissance au sein de la matière organique à partir d'un point formant les 'germes cristallins'. Ceux-ci, de forme généralement circulaire, croissent, se compriment et finissent par fusionner avec des germes cristallins voisins. L'orientation des fronts de minéralisation près des zones de croissance indique la direction de croissance des coquilles. Cinq zones de croissance (Z) ont été définies en fonction des figures dessinées par ces fronts. La couche nacrée des coquilles d'un mois ne montre aucune figure particulière (Z0) puis les fronts de minéralisation sont parallèles au bord des valves (Z1), ils deviennent sinueux (apparence d'empreintes digitales) (Z2) puis sont perpendiculaires au bord des coquilles (Z3). Une quatrième zone (Z4) caractérisée par des spirales de croissance s'ajoute aux trois autres zones, dans la région du crochet et est associée à un épaississement de la coquille. Ces résultats attestent d'un ralentissement de la minéralisation au cours du temps et d'un changement de la stratégie de croissance des bivalves. Une croissance en longueur est privilégiée chez les jeunes coquilles. Elle est ensuite remplacée par une stratégie d'épaississement chez les coquilles plus âgées. Les figures de minéralisation des coquilles d'écloserie sont similaires à celles du milieu naturel. Les informations sur la forme, la densité et la distribution des sites de nucléation en tant qu'indicateurs de croissance sont ici discutées. © 2001 Ifremer/CNRS/IRD/Éditions scientifiques et médicales Elsevier SAS

biomineralisation / nacreous layer / pearl oyster / *Pinctada margaritifera* / French Polynesia

biominéralisation / couche nacrée / huître perlière / *Pinctada margaritifera* / Polynésie française

1. INTRODUCTION

The nacreous (mother-of-pearl) layer of molluscs has attracted considerable interest and has been well studied. The first observations concerned the genus *Pinctada*, which is known to produce pearls, including the species *Pinctada fucata, P. martensii*, and *P. radiata* (Wada, 1961, 1965, 1972; Watabe, 1965, Bevelander and Nakahara, 1969, 1980; Nakahara and Bevelander, 1971; Iwata, 1975).

Pinctada margaritifera var. *cumingii*, which is of great economic importance in French Polynesia due to its production of black pearls was subject of numerous studies (Dauphin and Denis, 1987; Cuif et al., 1991; Dauphin and Cuif, 1991; Marin and Dauphin, 1991; Caseiro, 1993; Cuif and Dauphin, 1995). However, these studies mainly concerned the fine structure and biochemical aspects of adult shells, comparing normal and anomalous mineralisation products. The developmental aspects of the shell formation remain less known.

Progress in culturing techniques and the introduction of commercial pearl oyster hatcheries over the past two decades, offered the opportunity to follow the development of the shell formation from the planktonic larval stages to the adult and to determine the nature and timing of critical changes in the carbonate nucleation process. The work presented here is the first study on the development changes in fine structure during the course of shell formation from larval to adult stages.

2. MATERIAL AND METHODS

2.1. Study area

The shells used in this study originated from the atolls of Takapoto and Rangiroa, Tuamotu Archipelago (*figure 1*). Takapoto (14°30' S, 145°20' W) is the main centre of production of *Pinctada margaritifera*. The territorial shellfish hatchery was build in 1980 in the lagoon of Rangiroa (14°30' S, 147°40' W). However, a natural broodstock of pearl oysters does not exist on this atoll, so that fertile shells are imported from Takapoto and other atolls. In the Rangiroa hatchery, fertile oysters are introduced to spawn in tanks where collectors are immersed for the settlement of pediveligers. After three months, collectors are transferred to the lagoon of Rangiroa. After one year adult oysters are attached on ropes.

2.2. Material

The shells for this study represent different stages of development obtained at defined stages in the rearing
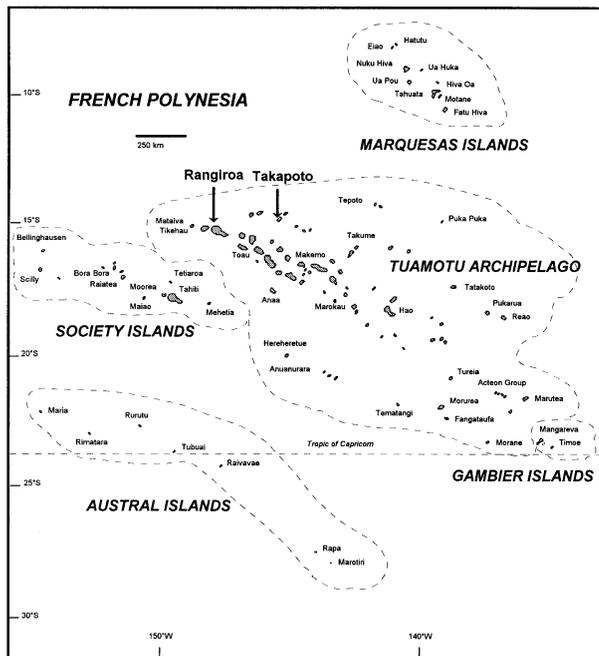
Figure 1. Location of sample sites on the Takapoto and Rangiroa atolls, Tuamotu Archipelago, French Polynesia.

process (summarized in *table I*). The following planktonic larval stages were obtained from the territorial hatchery at Rangiroa: D larvae, umboned larvae, eyed and pediveliger stages (*Service des Ressources Marines* unpublished). Spat up to 40 days old were obtained from a separate fertilization batch. Spat, 2 to 4 months old, and longer than 3 mm, were obtained from natural reproduction in the Takapoto lagoon. Juvenile and adult specimens were obtained from collectors exposed for one to two years in Takapoto lagoon.

2.3. Analytical procedures

2.3.1. Scanning Electron Microscopy (SEM)

We used Scanning Electron Microscopy (SEM) to observe the external surfaces of the shells after removal of organic matter by Na-hypochlorite. The nacreous surfaces were observed directly after opening the valves, washing them with distilled water, and after oven-drying for 3–6 h at 60 °C.

The nacreous layer was studied on shells at the dissochonch stage, approximately one month old, when the differentiation of the nacreous layer first occurs. Consid-

Table I. Main growth characteristics of the nacreous surface layer*.

Age	Zone	Number of crystalline bodies ($\times 10^{10}$ mm^{-2})	Size of crystaline bodies (µm)	Localization of nucleation site	Fusion
1 month	0	3.7 ± 1.13	1.7 ± 0.075	d	++
2 months	1	3.2 ± 0.158	2.32 ± 0.103	d	++
	2	2.39 ± 0.129	2.39 ± 0.16	d	++
	3	1.9 ± 0.147	1.86 ± 0.165	d	++
3 months	1	2.7 ± 0.133	2.2 ± 0.09	d	++
	2	2.4 ± 0.1	2.2 ± 0.192	d	++
	3	1.25 ± 0.119	1.9 ± 0.133	d	++
4 months	1	2.8 ± 0.22	2.1 ± 0.131	d	++
	2	2.3 ± 0.113	2.3 ± 0.135	d	++
	3	1.72 ± 0.105	2.46 ± 0.095	d	++
	4	0.72 ± 0.0717	2.93 ± 0.158	d	++
1 year	1	4.56 ± 0.372	1.6 ± 0.046	m	+++
	2	3.8 ± 0.347	1.8 ± 0.047	m	+++
	3	2.4 ± 0.263	2.6 ± 0.162	m	+++
	4	1.8 ± 0.22	2.67 ± 0.131	s	+
2 years	1	3.2 ± 0.23	1.85 ± 0.024	m	+++
	2	3.2 ± 0.18	2.18 ± 0.045	m	+++
	3	2.5 ± 0.2	2.68 ± 0.114	m	+++
	4	1.9 ± 93	3.5 ± 0.084	s	+

* Values are mean ± SD. Nucleation sites: d = distributed; m = marginal; s = superimposed. Crystal germ fusion: + = 0 to 20%; ++ = 20 to 50%; +++ = 50 to 100% fused.

ering their small diameter, whole valves of one- to four-month-old shells were observed under the microscope, directly after separation of the two valves. For observation of adult shells, a strip 1 cm wide was drawn along the length of the valve. Comparisons were made on the basis of 1-cm square areas designated along this strip, in order to monitor different growth strategies in the nacreous region.

2.3.2. Shell growth areas

For statistical evaluations, different growth areas of the shells beyond the dissoconch stage were subdivided in 5 zones: mineralisation fronts without particular figures (Z0), mineralisation fronts parallel to the growth edge of valves (Z1), curved and irregular mineralisation fronts (Z2), mineralisation fronts perpendicular to the growth edge of valves (Z3), and spiral growth of mineralisation fronts (Z4). The free 'crystal germs' (which do not show fusion with neighbouring crystals) were counted after SEM, using the screen area as a sampling unit at $3\,000 \times$ magnification as $1\,400\,\mu m^{-2}$ of surface. Eight screens were randomly chosen within each zone.

2.3.3. Density and size-frequency distribution of 'crystal germs'

The mean size and standard deviation, the density (expressed per mm^2), and the size-frequency distribution of 'crystal germs' were determined separately for each zone. Fused 'crystal germs' were estimated and classified into 4 categories: absent (–), 1 to 20% (+), 20 to 50% (++), and more than 50% of fused crystals (+++). Three shells are studied for each age class. Three types of localization of nucleation sites were recognized: (a) evenly spread between two mineralisation fronts, (b) limited to the front margin, and (c) on top of existing 'crystal germs'.

2.4. Statistical analysis

The comparison of mean values (after logarithmic transformations) for the densities and size of free 'crystal germs' was carried out by the two-way Analysis of Variance (ANOVA) with equal replication, completely randomized factorial design, fixed model. The factors retained were 'the age class': 3 levels (4 months, 1 year, 2 years) or 5 levels (2 months, 3 months, 4 months, 1 year, 2 years), and 'the nacre mineralisation zones': 3 levels (Z1, Z2, Z3) or 4 levels (Z1, Z2, Z3, Z4). These tests were complemented by means of the Student Newman Keuls (SNK) 'a posteriori' test (Zar, 1984). The relation between the mean size and the density of 'crystal germs' was obtained by Model II regression (reduced major axis, Sokal and Rohlf, 1995).

3. RESULTS

3.1. Mineralisation of developing shells

Prodissoconch-I, the first shell formed in the course of the veliger D-stage of larval development appears thin and transparent under a light microscope. The thickness of the larval shell is about 1.5 μm on the 6th day after fertilization. Both surfaces of the valves appear smooth and homogenous (figure 2a,b insert). Upon removal of the periostracum, the external mineral surface has a granular appearance with submicron size grains (0.1–0.3 μm) directionally oriented and grouped in cusps (figure 2b). Fractured surfaces do not show any organized texture.

Prodissoconch-II starts to develop approximately on the 17th day after fertilization. It is characterized externally by the appearance of concentric growth rings added to the margin of prodissoconch-I (figure 2c, arrow). The end of the prodissoconch-II stage, about 27–30 days after fertilization, is marked by the growth rings becoming closer together. The valves are still very thin. They measure in their central portion about 2–3 μm on the 17th day (in the umbo region they are up to 6 μm thick), and 6 μm on the 27th day. The granulation on the external surface of the mineral shell, following removal of the periostracum shows elongated fibers of 0.15–0.4 μm wide (figure 2d). The internal surface of the valves is smooth. Cross sections of the shell at different growth zones show an increased structural complexity. The prodissoconch-I part of the shell (umbo region), a thin layer of short parallel-organized prisms is added internally to the structureless prodissoconch shell (figure 2e). The newly added shell (concentric rings) is well organized in columns of long parallel prisms perpendicular to the surface (figure 2f). At the growing edge of the new shell, however, the fractured surfaces again appear without defined texture (figure 2g). This stage immediately precedes the onset of the nacreous layer formation, which coincides with the larval settlement and marks the beginning of the metamorphosis.
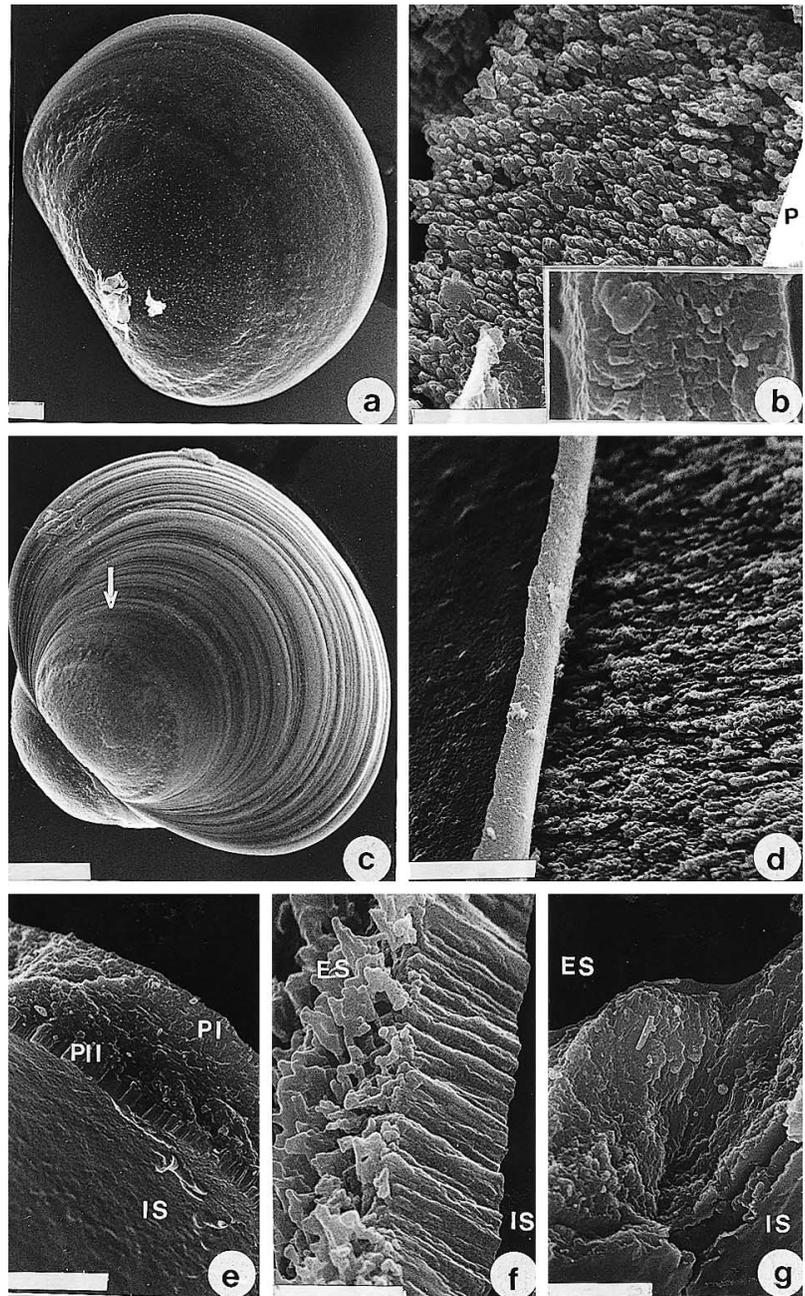
Figure 2. Larval shells. (a) Prodissoconch-I. The surface is smooth due to the periostracum cover. Scale bar = 10 μm. (b) Granular texture organized in pointed cusps of the mineral part of the prodissoconch-shell after removal of the periostracum (P). Insert: fractured prodissoconch-shell with undefined texture. Scale bar = 5 μm for both. (c) Prodissoconch-II characterized by concentric growth rings added to prodissoconch I shell. The contact between prodissoconch I and II is marked by an arrow. Scale bar = 50 μm. (d) Fibrous texture of the mineral part of the prodissoconch-II shell after removal of the periostracum. Scale bar = 5 μm. (e) Prodissoconch-II shell fractured at the umbo region showing the columnar organization of prodissoconch-II (PII) on the interior side of the shell (IS) added to the undifferentiated prodissoconch-I (PI) deposit. Scale bar = 5 μm. (f) Fracture in the middle of the prodissoconch-II shell showing the prismatic organization. The interior surface (IS) is smooth, while the external one (ES) is rugged (when periostracum is removed). Scale bar = 2 μm. (g) Fracture at the growing edge of the Prodissoconch-II shell. Note the lack of organization of the carbonate deposit. Scale bar = 5 μm.

Dissoconch is the adult shell, it develops in young settled oysters approximately 1 month after fertilization. In a 40-day-old shell a distinct transition or metamorphosis line (*figure 3a*) links the larval prodissoconch (P) with the dissoconch shell (D). Fractured surfaces at this stage show that all elements of an adult shell are already present (*figure 3b*). The outer mineral region consists of a layer of short prisms (PL) followed by a less-defined transition layer. The internal surface is lined by a young nacreous region of several layers of superimposed aragonitic tablets. In the plane view of the interior surface the bases of the prisms are visible along the outer edge of the shell (*figure 3c*, PL). They can reach up to 28 μm in diameter. The nacreous (NL) layer, characterized by

numerous rounded nucleation centres, covers the rest of the interior surface. It is characterized by scattered, rounded to oblong 'crystal germs' of variable sizes, which fuse together. A smooth contiguous belt at the contact between the prismatic and nacreous region represents the transition zone.

3.2. Mineralisation and growth of the nacreous layer

The formation of the nacreous layer marks the beginning of the metamorphosis. SEM observations of internal surfaces reveal ultrastructural differences in shells of different ages, but also in different parts of the same shell. In one-month-old shells, only one homogeneous zone (Z0) coats the interior surface of valves, which is speckled with evenly distributed rounded 'crystal germs' (*figure 4a*). These nucleation sites appear at different levels and are of variable size (*figure 4b*).

During the second month, the uniform appearance of the internal nacreous surface, is replaced by a scalariform arrangement of additional calcification layers, in which new nucleation sites appear in linear fronts. Three different patterns in the orientation of these mineralisation fronts could be observed. They are arranged in concentric zones from the growing edge (ventral) towards the hinge (dorsal) area. The first zone (Z1) of mineralisation fronts is characterized by scalariform rows parallel to, and descending toward the growing edge (*figure 4c*). In the second zone (Z2), the rows start to wind irregularly, resembling finger prints, to turn predominantly perpendicular to the growing edge in the third, interior zone (Z3).

In two- and three-month-old shells, the detailed arrangement of nucleation sites on the surface of each step is the same in all three zones. The 'crystal germs' are numerous and cover a wide range of sizes. They are circular to oblong in shape with the longitudinal axis often parallel to the stairs edge. They expand until they fuse together into a contiguous smooth surface (*figure 4d*). This detailed pattern changes for one- and two-year-old shells. The number of nucleation centres is markedly reduced, although the orientation of the mineralisation fronts in different zones remains the same (*figure 5a*). The edges of the stairs in all three zones show mostly large rounded 'crystal germs', most of them in different stages of fusion.
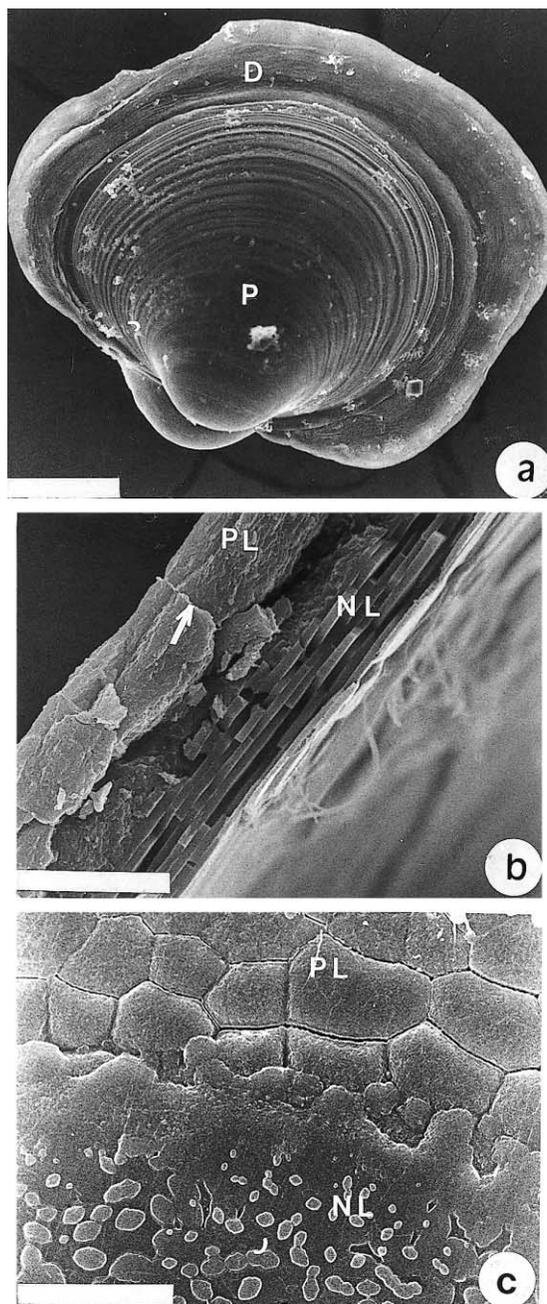
Figure 3. Spat dissoconch. (a) The shape of the shell showing dissoconch portion (D) added to the prodissoconchs. Scale bar = 100 μm. (b) Fractured one-month-old shell from the hatchery showing the formed prismatic region (PL) composed of a layer of short prisms and a nacreous region (NL) composed of several layers of aragonite platelets. Scale bar = 10 μm. (c) Detail of the internal surface of the shell showing the interface between the prismatic layer (PL) and nacreous layer (NL) in plane view. Note the numerous circular and oblong 'crystal germs' scattered over a smooth background. Scale bar = 30 μm.

Figure 4. Nacreous surface of the young dissoconch. (a) Planar view of the undifferentiated (Z0) zone at the edge of the one-month-old hatchery shell. Note the random distribution of 'crystal germs' of various sizes. Scale bar = 60 μm. (b) Detail of the internal nacreous surface (a), with a wide range of sizes of free and fused 'crystal germs'. Scale bar = 10 μm. (c) Inner surface of the two-month-old shell. Mineralisation fronts are clearly linear, differentiated in three zones with different orientations: Z1 zone has stairs descending parallel to the ventral, growing edge, Z2 with curved, finger-print like patterns and Z3 oriented perpendicular to the shell's edge. Scale bar = 150 μm. (d) Detail of (c) with regularly aligned sequence of 'crystal germs', starting with a row of initial nucleation centres gradually increasing in size and fusing into the next higher nacreous level. Scale bar = 20 μm.
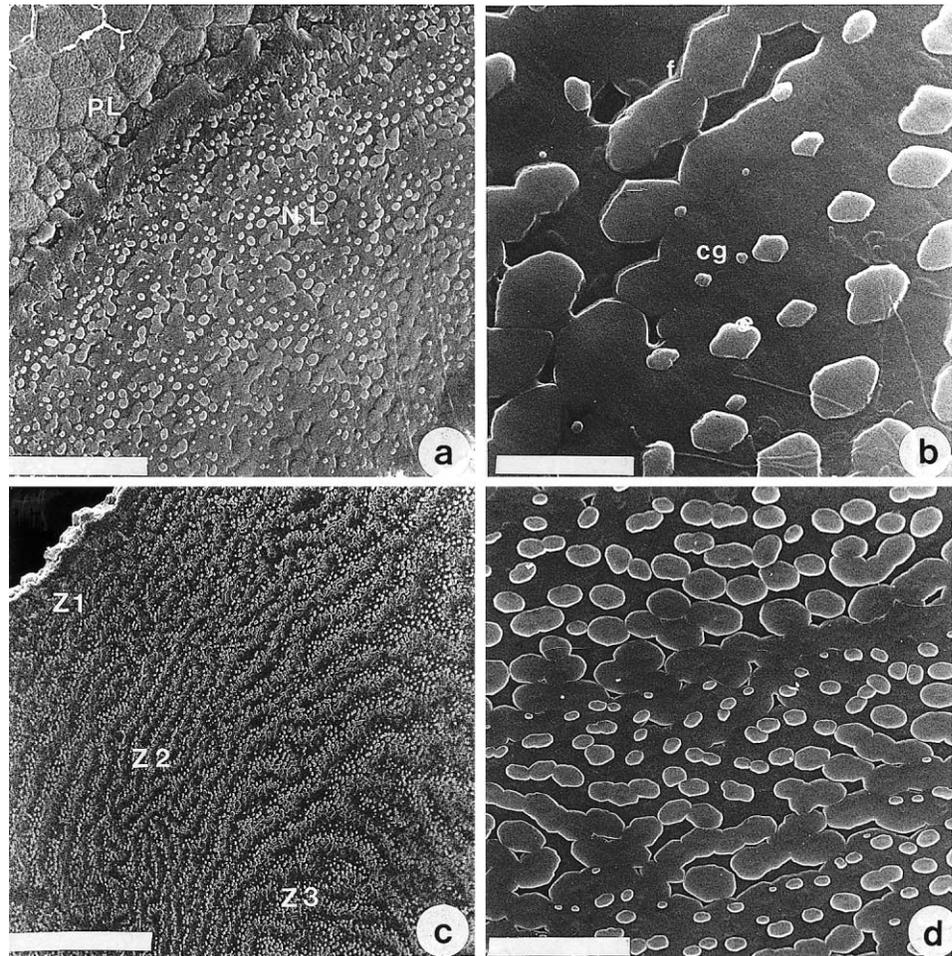
There are hardly any new nucleation points appearing on the surfaces of the next lower level (*figure 5b*).

In shells up to 4 months old, a 4th zone (Z4) is added beyond the zone 3, from the area of the muscle attachment to the umbo of the shell. This zone is characterized by the formation of ascending spirals (Wada, 1961). The arrangement of nucleation fronts form a three-dimensional terraced landscape (*figure 5c*). Higher magnification reveals a less regular arrangement of 'crystal germs' of different sizes occurring simultaneously at different levels (*figure 5d*).

3.3. Density of 'crystal germs'

The density of 'crystal germs' was determined on the basis of free-standing units; fused 'crystal germs' were ignored. The one-month-old shells have not been included in the two-factor ANOVA testing because they do not show differentiation between the zones. The density of nucleation sites is high ($3.7 \times 10^{10} \pm 1.13 \times 10^{10}$ mm^{-2}). Results of the ANOVA (*figure 6c,d*) show that the crystal density varies with the age and zones being considered ($P = 0.0001$ for the 2 factors). The Student Newman Keuls (SNK) test results show a reduction in the number of free nucleation sites for shells of all ages from the edge toward the interior (*figure 6a*). The same tendency continues for the 4 zones in older shells between 4 months and 2 years (*figure 6b*). Hence, for four-month-old shells, the density of nucleation sites decreases from 2.8×10^{10} mm$^{-2} \pm 2.2 \times 10^{10}$ mm^{-2} (Z1) to 1.72×10^{10} mm$^{-2} \pm 1.05 \times 10^{10}$ mm^{-2} within Z3, and 7.2×10^{10} mm$^{-2} \pm 7.17 \times 10^{8}$ mm^{-2} within Z4. This decrease is less important for one- and two-year-old
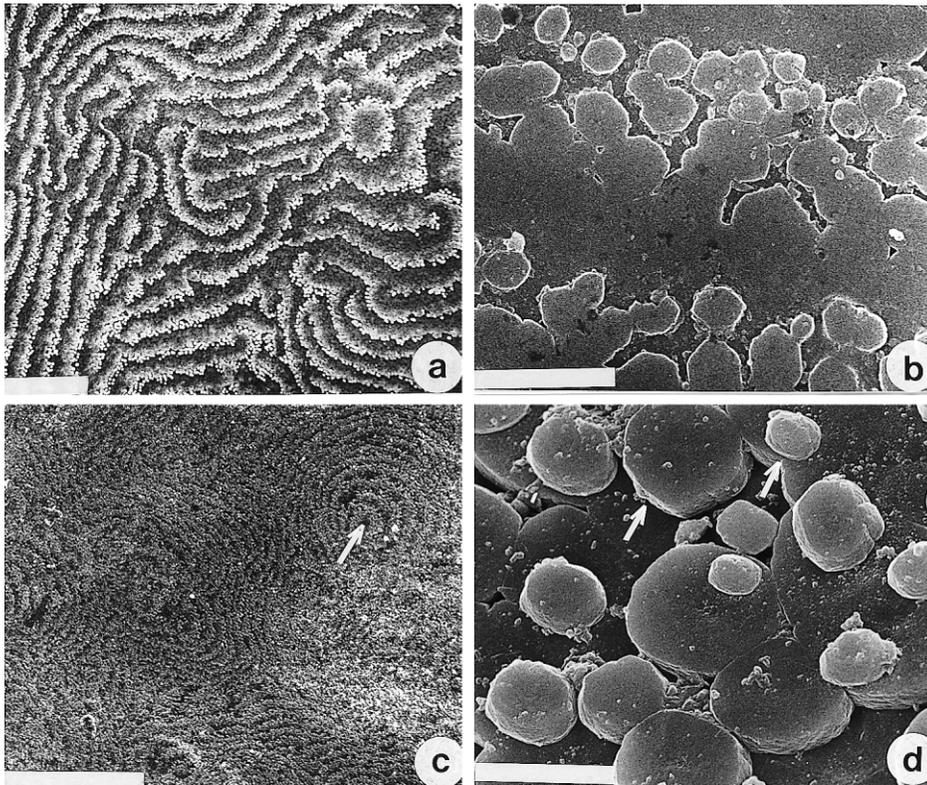
Figure 5. Nacreous surface of the adult two-year-old shell. (a) Labyrinthic (finger print) arrangement of mineralisation fronts in the Z3 zone (see *figure 5c*). Scale bar = 100 µm. (b) Detail of (a) Note the paucity of free 'crystal germs'; a smooth surface extends between two fronts of fused germs. Scale bar = 10 µm. (c) Zone 4 of the nacreous surface in the umbo region of an adult shell showing a three-dimensional contoured landscape with several loci with spiral growth. Scale bar = 300 µm. (d) Detail of zone 4. The 'crystal germs' are superimposed on each other promoting simultaneous mineralisation at several levels and contributing to the growth in thickness of the shell. Scale bar = 10 µm.

shells. The SNK test also confirms that the nucleation site density in one-year-old shells is higher than in two-year-old ones which, in turn, is higher than in shells of 2, 3, and 4 months respectively. Interaction graphs (*figure 7a,b*) reveal that the density within Z1 of one-year-old shells is higher than in two-year-old shells.

3.4. The size of 'crystal germs'

Figure 7 shows that in one- to four-month-old juveniles, the sizes of the 'crystal germs' are broadly distributed over a range between 0 and 5 mm in all three zones. In older, one- to two-year-old shells, the distribution shows dominant peaks for the zones 1 and 2 in the 1-mm range, and for the zone 3 in the 2–3 mm range. The zone 4, which is added from the fourth month on, consistently has a broad-size distribution range with dominance in the 2–4 mm range, but over time it looses the small-size component.

The results of the two ANOVA tests indicate that mean sizes of 'crystal germs' vary in relation to their age and the strata ($P < 0.05$ in every case, *figure 8c,d*). Interactions are also very significant ($P = 0.0001$). *Figure 8a* representing the three firsts zones of all shells, shows that the size of the 'crystal germs' increases from Z1 to Z2, except for three-month-old shells. However, if we consider the 3 zones, 2 general trends can be noticed: the general tendency in shells older than 4 months is that the average size gradually increases between the zones 1 and 3 (opposite from density). This observation can be extended to Z4 (*figure 8b*). Exceptions are the younger shells, which show a decrease in the average size of 'crystal germs' (*figure 8a*).

3.5. Relationship between the density and size of 'crystal germs'

Linear regressions between the mean crystal germ sizes (x) and the density (y) have been performed for the two groups. Results are shown in *figure 9*. During the second and third month, the relationship between the two parameters is positive: $y = 3.211 \times 10^{-11} x + 1.353$ ($R = 0.85$, $P < 0.05$) (*figure 9a*). This result confirmed previ-
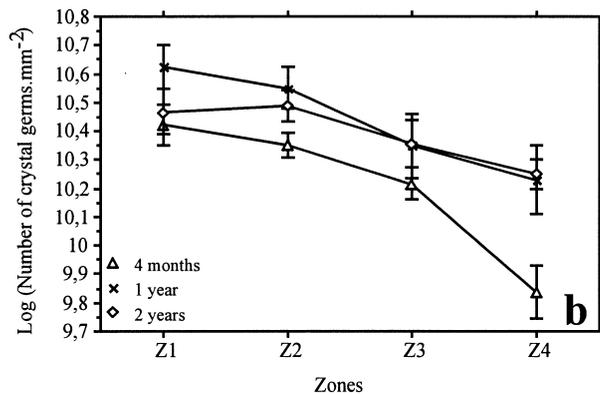
Figure 6. Log of number of 'crystal germs' per mm^2 for different mineralisation zones (means ± SD, $n = 24$) shown as vertical bars for shells of different ages (see legend). (a) Three zones for age classes from two months to two years. (b) Four zones for age classes from four months to two years. (c,d) Two-way Analysis of Variance for Log density of 'crystal germs' vs. age and mineralisation zone. df = degrees of freedom; MS = Mean Square; F = F ratio; P = probability

ous observations: the external zone (Z1) has a larger number of big 'crystal germs' while the centre (Z3) has a rather low number of small 'crystal germs'. As of the 4th month, the trend reverses. The relationship is negative and expressed by $y = -5.396 \times 10^{-11} x + 3.802$ ($R = 0.89$, $P < 0.001$) (*figure 9b*). For shells older than 4 months, the growing edge is characterized by a large number of small 'crystal germs'. The central zones, on the other hand, are characterized by a small number of large 'crystal germs'.

Most 'crystal germs' observed in our study are circular to oval in shape. Only 6 samples out of 50 shells studied contained euhedral or corroded 'crystal germs' (Wada, 1961). These were encountered randomly at different seasons. The same 'crystal germ' shapes were found in shells from a natural habitat and in those from culture. The results of this study are summarized in *table I*.

4. DISCUSSION

We have observed and statistically verified significant differences in the number, density, and arrangement of mineral nucleation centres and of mineralisation fronts in different developmental stages, as well as in different growth areas of the shell. The observed differences are therefore likely to reflect different growth strategies in the course of shell development.

4.1. Process of calcification

It has been suggested that differences in calcification in different parts of the shell may reflect minor differences in the chemical composition of the extrapallial fluid caused by currents produced by movements and length-
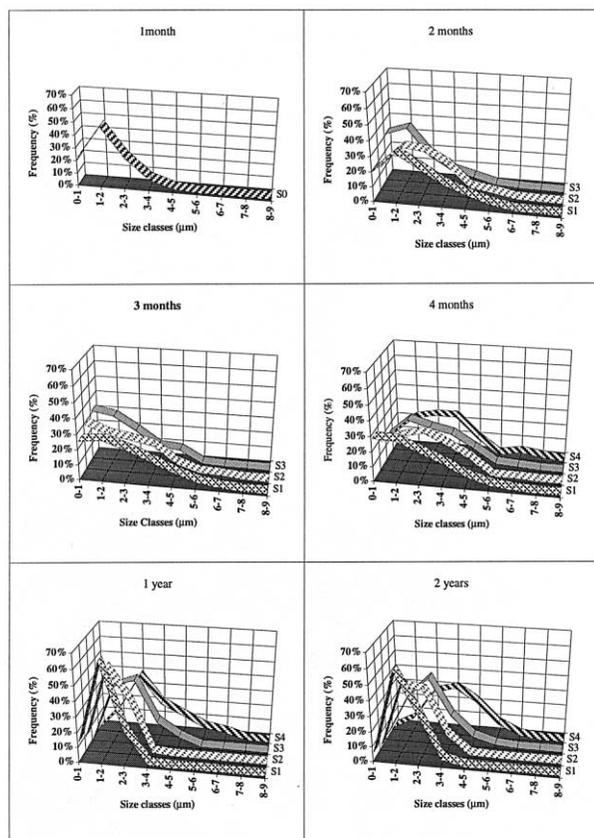
Figure 7. Size frequency distribution (%) of 'crystal germs' in relation to size classes, for different zones (Z0-Z4) and age classes.

ening of the mantle, without a need for any functional differentiation of the latter (Wada, 1972). However, complex spatial and temporal differentiation of the mantle tissue has also been suggested for *Ostrea edulis* (Waller, 1980). These two different views appear to be complementary. The influences of the mantle tissue on calcification is in any case indirect, since the actual nucleation of calcium carbonate always takes place within an organic matrix laid down by the mantle (Bevelander and Nakahara, 1969; Wilbur, 1972). Our observations are consistent with the view that different parts of the mantle are involved at different times in secreting first prodissoconch-I, then prodissoconch-II, and dissoconch. The mantle tissue, which produces the mature shell is then subdivided in a portion involved in the formation of calcitic prismatic layers and a portion involved in the formation of the nacre (Waller, 1980).

In *P. martensii*, the two larval shells, prodissoconch-I and -II are composed of dahlite and calcite, respectively (Watanabe, 1956). The other view (Wada, 1961) is that the two larval shells are of different mineral composition and differ also from adult shells. Crystallographic characteristics have been studied in different developmental stages of other bivalves. In *Crassostrea virginica*, for example, the two prodissoconchs are aragonitic while the adult shell is entirely calcitic, except for the myostracum (Carriker and Palmer, 1979). These observations agree
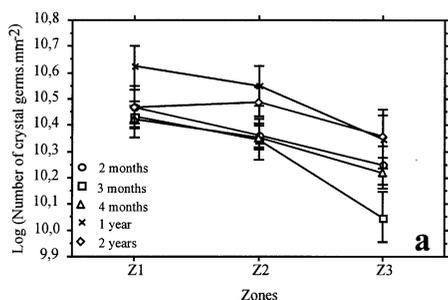
Source of variation	df	MS	F	P
Factor A (Age)	4	0.583	18.953	0.0001
Factor B (Zone)	2	1.876	61.004	0.0001
Interaction (AXB)	8	0.080	2.588	0.0092
Residual (error)	371	0.031		
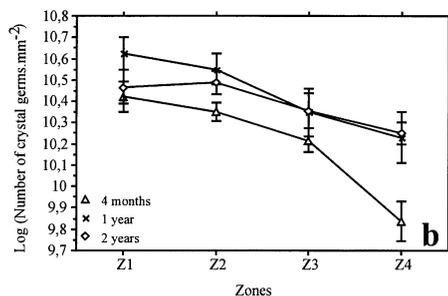
Source of variation	df	MS	F	P
Factor A (Age)	2	1.347	41.427	0.0001
Factor B (Zone)	3	2.122	65.336	0.0001
Interaction (AXB)	6	0.190	5.851	0.0001
Residual (error)	288	0.032		

Figure 8. Interaction graphs between the two factors (age, zone) and their mean effects. Log of 'crystal germ' sizes in μm (mean ± SD, $n = 100$) in relation to mineralisation zones. (a) Three zones for age classes from two months to two years. (b) Four zones for the age classes from 4 months to 2 years. (c,d) Two-way Analysis of Variance for Log crystal germ size (μm) vs. age and mineralisation zone. df = degrees of freedom; MS = Mean Square; F = F ratio; P = probability.

(a)

$y = 3{,}211.10^{-11}x + 1{,}353$
$R^2 = 0{,}654$
$R = 0{,}85$

(b)

$y = -5{,}396.10^{-11}x + 3{,}802$
$R^2 = 0{,}79$
$R = 0{,}89$
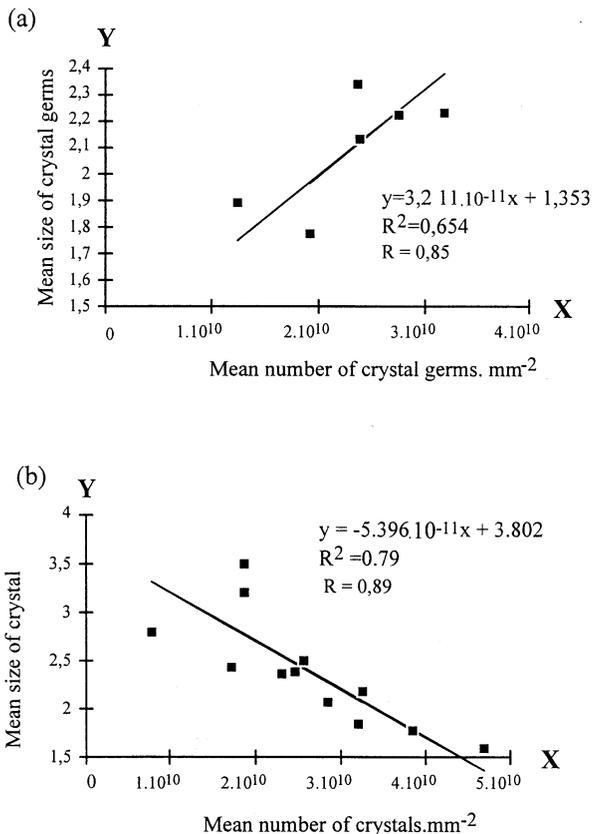
Figure 9. Linear regression (reduced major axis) between mean size and density of crystals for shells of different ages. (a) Two and three months. (b) Four months, one and two years.

with those that claim that practically all larval shells of bivalves are aragonitic (Stenzel, 1964). In our observations the elongated to fibrose crystals of larval shells (*figures 2b,d*) are morphologically similar to marine fibrous aragonite deposited in some prokaryotic systems (Golubic and Campbell, 1981; Golubic, 1983).

4.2. Process of growth

Young shells (less than 3 months old) have areas characteristic for a fast growth rate. In this case, the nacreous internal surface has numerous crystals of small diameter (0–2 μm class is dominant) whose great number is coalescent.

Four- month-old shells show two different areas: a marginal area grouping three zones whose mineralisation

fronts can be parallel to the growing edge, and a central area beyond the muscular insertion, characterized by growth spirals. These observations clearly illustrate a differentiation of epithelial cells for each zone of the shell.

The marginal areas are characteristic of areas with a high growth rate (numerous small 'crystal germs' coalescent). The absence of superimposition of mineralisation levels suggests an essentially diameter-wise growth, probably as a result of a lengthening of the mantle (Waller, 1980). The central areas, meanwhile, are characteristic for areas with a low growth rate, with few large-diameter crystals. The simultaneous existence of several levels of mineralisation and of numerous sites of nucleation lead to a thickening of the shell. The presence of spiral growth in the shells' central areas confirms this hypothesis. According to the spiral-growth model (Wada, 1961), spiral growth figures observed in the central areas of adult *P. martensii* shells, characterize areas where growth is slowed down.

4.3. Rate of carbonate precipitation

In our observations no crystal fabrics were evident in growing 'crystal germs', not even when the organic coating was removed and high-resolution SEM was applied to submicron details. Faint granular surface irregularities were observed only in the centres of these carbonate deposits. This implies that the rate of carbonate precipitation in the nucleation centres is too rapid for an organized crystal growth and that this carbonate deposit is initially amorphous. Recrystallization starts with a delay from the centre of the deposit and moves outward. This explanation is consistent with the view that rounded 'crystal germs' indicate high, and euhedral ones low, rates of precipitation, the latter allowing a crystallographic organization during deposition (Wada, 1972; Lutz and Rhoads, 1977).

4.4. Seasonal influence on carbonate precipitation

P. martensii from temperate regions show seasonal changes in the deposition of $CaCO_3$ with a maximum calcification rate during the warm season at temperatures between 20 and 29 °C (Wada, 1961, 1972). During this period, small-diameter 'crystal germs' (2–4 μm) of a rounded shape are numerous. During the cold season, at

temperatures between 11 and 19 °C, growth slows down, and the aragonite 'crystal germs' have larger diameter (4–7 µm) and euhedral outlines. At temperatures below 8 °C growth ceases, and the aragonite crystals are subjected to corrosion, probably linked to acidification of the extrapallial fluid and anaerobic metabolism (Lutz and Rhoads, 1977, 1980).

In this study pearl oysters were collected during the hot season (November to April) as well as in the cool season (May to October). The occurrence of crystals with euhedral shapes and corroded outlines were encountered during the southern winter (July), the southern summer (January), and also during the mid-seasons (April and September), for shells of different ages (one month to three years). The 'crystal germs' were almost always rounded. Less then 10% of the shells contained euhedral, and less than 2% corroded 'crystal germs'.

In the Tuamotu Archipelago, the temperature of the lagoon sea water varies annually from 26 to 30 °C (Rougerie, 1979; Buestel and Pouvreau, 1994). Thus, different shapes of crystals observed are unlikely to depend on environmental temperature changes and may instead reflect the physiological state of individual animals. If so, the shape of the 'crystal germs' may be used as a practical method for the estimation of growth conditions in pearl oyster culturing. The presence of numerous shells with euhedral or corroded 'crystal germs' in a farm may reflect problems with the growth conditions.

Acknowledgements

REFERENCES

Bevelander, G., Nakahara, H., 1969. An electron microscope study of the formation of the nacreous layer in the shell of certain bivalve molluscs. Calc. Tiss. Res. 3, 84–92.

Bevelander, G., Nakahara, H., 1980. Compartment and envelope formation in the progress of biological mineralisation. In: Omori, M., Watanabe, N. (Eds.), Tokyo Proc. 3th Inter. Biomin. Symp., The Mechanisms of Biomineralisation in Animals and Plants. Tokai University Press, Tokai, pp. 19–27.

Buestel, D., Pouvreau, S., 1994. Ecophysiologie de l'huître perlière – Approche des relations entre la croissance de l'huître Pinctada margaritifera et le milieu lagonaire de Takapoto, Rapport P.G.R.N. Ifremer, Plouzané.

Carriker, M.R., Palmer, R.E., 1979. Ultrastructural morphogenesis of prodissoconch and early dissoconch valves of the oyster Crassostrea virginica. Proc. Nat. Shellfish. Ass. 69, 103–128.

Caseiro, J., 1993. L'huître perlière de Polynésie. Biominéralisation, paramètres et processus de croissance, effets chromatiques dans la coquille et la perle de Pinctada margaritifera, PhD Thesis. Université Claude-Bernard–Lyon I, Lyon.

Cuif, J.P., Dauphin, Y., 1995. Disturbed mineralisation process in shells and pearls of Pinctada margarifera from French Polynesia. Microstructural and biochemical patterns, Intern. Workshop on Shell Disease in Marine Invertebrates: Environment-host-pathogen interactions.

Cuif, J.P., Dauphin, Y., Denis, A., Jaillard, L., Marin, F., 1991, Aspect et caractéristiques biochimiques des cristaux, Rapport CORDET 88/210: Pinctada margaritifera, le manteau, ses altérations en Polynésie.

Dauphin, Y., Cuif, J.P., 1991. Epizootic disease in the 'black lip' pearl oyster Pinctada margaritifera in French Polynesia: Ultrastructural alterations of the nacreous layer. In: Suga, S., Nakahara, H. (Eds.), Biomineralisations: Patterns, Processes and Evolutionary Trends. Springer–Verlag, New York, pp. 67–171.

Dauphin, Y., Denis, A., 1987. Altération microstructurale de la nacre des huîtres perlières (Pinctada margaritifera) atteintes par l'épizootie en Polynésie française. C.R. Acad. Sci. Paris 305, 649–654.

Golubic, S., 1983. Stromatolites, fossil and recent: a case of history. In: Westbroek, P., Dejong, E.W. (Eds.), Biomineralisation and biological metal accumulation. D. Reidel Publ., Dordrecht, pp. 1–14.

Golubic, S., Campbell, S.E., 1981. Biogenically formed aragonite concretions in marine Rivularia. In: Monty, C.L.V. (Ed.), Phanerozoic Stromatolites. Springer–Verlag, New York, pp. 209–229.

Iwata, K., 1975. Ultrastructure of the condition matrices in molluscan nacreous layer. J. Fac. Sci Hokkaido Univ. IV 17, 173–229.

Lutz, R.A., Rhoads, D.C., 1977. Anaerobiosis and a theory of growth line formation. Micro and ultra-structural growth patterns within molluscan shell reflect periodic respiratory change. Science 198, 1222–1227.

Lutz, R.A., Rhoads, D.C., 1980. Growth patterns within the molluscan shell: An overview. In: Rhoads, D.C., Lutz, R.A. (Eds.), Skeletal Growth of Aquatic Organisms. Plenum Publishing Co., New York, pp. 203–254.

Marin, F., Dauphin, Y., 1991. Diversité des altérations dans la composition en acides aminés de la phase organique de la nacre des huîtres perlières de Polynésie Française (*Pinctada margaritifera*) atteintes par l'épizootie. C.R. Acad. Sci. Paris 312, 483–488.

Nakahara, H., Bevelander, G., 1971. The formation and growth of the prismatic layer of *Pinctada radiata*. Calc. Tiss. Res. 7, 31–45.

Rougerie, F., 1979. Caractéristiques générales du milieu liquide lagonaire de l'atoll de Takapoto. J. Soc. Océan. 62, 35–45.

Sokal, R.R., Rohlf, F.J., 1995. Biometry, The principles and practice of statistics in biological research. Freeman and Co., San Francisco.

Stenzel, H.B., 1964. Oysters: composition of the larval shell. Science 145, 155–156.

Wada, K., 1961. Crystal growth of molluscan shells. Bull. Nat. Pearl Res. Lab. 36, 703–869.

Wada, K., 1965. Studies on shell formation. XI. Crystal matrix relationships on the inner layers of mollusk shells. J. Ultrastr. Res. 12, 351–370.

Wada, K., 1972. Nucleation and growth of aragonite crystals in the nacre of some bivalve molluscs. Biomineralisation 6, 141–159.

Waller, T.R., 1980. Scanning electron microscopy of shell and mantle in the order arcoida (Mollusca: Bivalvia), Smithsonian Contrib. Zool. 328. Smithsonian Institution Press, Washington, DC.

Watabe, N., 1965. Studies on shell formation XI. Crystal matrix relationships in the inner layers of mollusk shells. J. Ultrastr. Res. 12, 351–370.

Watanabe, N., 1956. Dahllite identified as a constituent of Prodissoconch I of *Pinctada martensii* (Dunker). Science 124, 630.

Wilbur, K.M., 1972. Shell formation in mollusks. In: Florkin, M., Sheer, B. (Eds.), Mollusca Chemical Zoology. Academic Press, New York, pp. 103–145.

Zar, J.H., 1984, Biostatistical Analysis, 2th edition. Prentice–Hall, Englewood Cliffs, p. 718.